Waveguiding in nanoscale metallic apertures

Stéphane Collin, Fabrice Pardo and Jean-Luc Pelouard

Laboratoire de Photonique et de Nanostructures (LPN-CNRS)
Route de Nozay, 91460 Marcoussis, France

stephane.collin@lpn.cnrs.fr

Abstract: We study the optical properties of subwavelength metallic waveguides made of nanoscale apertures in a metal. We develop analytical expressions for the fundamental optical modes in apertures. The results are in excellent agreement with finite element calculations. This model provides a physical understanding of the role of non-perfect metallic walls, and of the shape and size of the apertures. They reveal the effect of the skin depth and of the surface plasmon polariton coupling on the waveguide modes. The nanoscopic origin of the increase of the cut-off wavelength due to the electromagnetic penetration depth in the metal is described. Simple expressions and universal curves for the effective index and the cut-off wavelength of the fundamental guided mode of any rectangular metallic waveguide are presented. The results provide an efficient tool for the design of nanoscale waveguides with real metal.

OCIS codes: (230.7370) Waveguides; (240.6680) Surface plasmons; (260.3910) Metals, optics of; (260.2110) Electromagnetic theory

References and links

1. T. W. Ebbesen, H. J. Lezec, H. F. Ghaemi, T. Thio, P. A. Wolff, "Extraordinary optical transmission through sub-wavelength hole arrays," Nature (London) **667,** 391 (1998).
2. William L. Barnes, Alain Dereux and Thomas W. Ebbesen, "Surface plasmon subwavelength optics," Nature (London) **824,** 424 (2003).
3. Hervé Rigneault, Jérémie Capoulade, José Dintinger, Jérôme Wenger, Nicolas Bonod, Evgeni Popov, Thomas W. Ebbesen, and Pierre-Franois Lenne "Enhancement of Single-Molecule Fluorescence Detection in Subwavelength Apertures," Phys. Rev. Lett. **95,** 117401 (2005).
4. H. J. Lezec, A. Degiron, E. Devaux, R. A. Linke, L. Martin-Moreno, F. J. Garcia-Vidal, and T. W. Ebbesen, "Beaming Light from a Subwavelength Aperture," Science **297,** 820 (2002).
5. D. E. Grupp, H. J. Lezec, T. Thio, and T. W. Ebbesen "Beyond the Bethe Limit : Tunable Enhanced Light Transmission Through a Single Sub-Wavelength Aperture," Adv. Mat. **11,** 860 (1999).
6. Tineke Thio, K. M. Pellerin, R. A. Linke, H. J. Lezec, and T. W. Ebbesen, "Enhanced light transmission through a single subwavelength aperture," Opt. Lett. **26,** 1972 (2001).
7. A. Degiron, H.J. Lezec, N. Yamamoto, and T.W. Ebbesen, "Optical transmission properties of a single subwavelength aperture in a real metal," Opt. Commun. **239,** 61 (2004).
8. Francisco Garcia de Abajo, "Light transmission through a single cylindrical hole in a metallic film," Opt. Express **10,**, 1475 (2002).
9. F. J. García-Vidal, Esteban Moreno, J. A. Porto, and L. Martín-Moreno "Transmission of Light through a Single Rectangular Hole," Phys. Rev. Lett. **95,** 103901 (2005).
10. Evgeny Popov, Michel Nevière, Philippe Boyer, and Nicolas Bonod, "Light transmission through a subwavelength hole," Opt. Commun. **255,** 338 (2005).
11. F. J. García-Vidal, L. Martín-Moreno, Esteban Moreno, L. K. S. Kumar, and R. Gordon "Transmission of light through a single rectangular hole in a real metal," Phys. Rev. B **74,** 153411 (2006).
12. N. M. Arslanov, "The optimal form of the scanning near-field optical microscopy probe with subwavelength aperture," J. Opt. A **8,** 338 (2006).

#78453 - $15.00 USD Received 22 December 2006; revised 2 February 2007; accepted 6 February 2007

13. M. J. Levene, J. Korlach, S. W. Turner, M. Foquet, H. G. Craighead, and W. W. Webb, "Zero-Mode Waveguides for Single-Molecule Analysis at High Concentrations," Science **299,** 682 (2003).
14. L. Martín-Moreno, F. J. Garcia-Vidal, H. J. Lezec, K. M. Pellerin, T. Thio, J. B. Pendry and T. W. Ebbesen, "Theory of Extraordinary Optical Transmission through Subwavelength Hole Arrays," Phys. Rev. Lett. **86,** 1114 (2001).
15. P. Lalanne, J.-C. Rodier, and J.-P. Hugonin, "Surface plasmons of metallic surfaces perforated by nanohole arrays," J. Opt. A **7,** 422 (2005).
16. J. B. Pendry, L. Martín-Moreno, and F. J. Garcia-Vidal, "Mimicking Surface Plasmons with Structured Surfaces," Science **305,** 847 (2004).
17. F. J. Garcia-Vidal, L. Martín-Moreno, and J. B. Pendry, "Surfaces with holes in them: new plasmonic metamaterials," J. Opt. A **7,** S97 (2005).
18. K. J. Klein Koerkamp, S. Enoch, F. B. Segerink, N. F. van Hulst, and L. Kuipers "Strong Influence of Hole Shape on Extraordinary Transmission through Periodic Arrays of Subwavelength Holes," Phys. Rev. Lett. **92,** 183901 (2004).
19. K. L. van der Molen, F. B. Segerink, N. F. van Hulst, and L. Kuipers "Influence of hole size on the extraordinary transmission through subwavelength hole arrays," Appl. Phys. Lett. **85,** 4316 (2004).
20. K. L. van der Molen, K. J. Klein Koerkamp, S. Enoch, F. B. Segerink, N. F. van Hulst, and L. Kuipers "Role of shape and localized resonances in extraordinary transmission through periodic arrays of subwavelength holes: Experiment and theory," Phys. Rev. B **72,** 045421 (2005).
21. A. Degiron, and T. W. Ebbesen, "The role of localized surface plasmon modes in the enhanced transmission of periodic subwavelength apertures," J. Opt. A **7,** S90 (2005).
22. J. A. H. van Nieuwstadt, M. Sandtke, R. H. Harmsen, F. B. Segerink, J. C. Prangsma, S. Enoch, and L. Kuipers, "Strong Modification of the Nonlinear Optical Response of Metallic Subwavelength Hole Arrays," Phys. Rev. Lett. **97,** 146102 (2006).
23. J. A. Porto and F. J. Garcia-Vidal and J. B. Pendry, "Transmission Resonances on Metallic Gratings with Very Narrow Slits", Phys. Rev. Lett. **83,** 2845 (1999).
24. L. Martín-Moreno, and F. J. Garcia-Vidal, "Optical transmission through circular hole arrays in optically thick metal films", Opt. Express **12,** 3619 (2004).
25. P. Lalanne, and J.-P. Hugonin, "Interaction between optical nano-objects at metallo-dielectric interfaces," Nat. Mater. **2,** 509 (2006).
26. F.I. Baida, D. Van Labeke, G. Granet, A. Moreau, and A. Belkhir, "Origin of the super-enhanced light transmission through a 2-D metallic annular aperture array: a study of photonic bands," Appl. Phys. B **79,** 1 (2004).
27. Commercial software (Femlab/Comsol).
28. L. Novotny, and C. Hafner "Light propagation in a cylindrical waveguide with a complex, metallic, dielectric function," Phys. Rev. E **50,** 4094 (1994).
29. Hocheol Shin, Peter B. Catrysse, and Shanhui Fan "Effect of the plasmonic dispersion relation on the transmission properties of subwavelength cylindrical holes," Phys. Rev. B **72,** 085436 (2005).
30. K. J. Webb and J. Li "Analysis of transmission through small apertures in conducting films," Phys. Rev. B **73,** 033401 (2006).
31. Reuven Gordon, and Alexandre G. Brolo, "Increased cut-off wavelength for a subwavelength hole in a real metal," Opt. Express **13,** 1933 (2005).
32. Jirun Luo and Chongqing Jiao "Effect of the lossy layer thickness of metal cylindrical waveguide wall on the propagation constant of electromagnetic modes," Appl. Phys. Lett. **88,** 061115 (2006).
33. F. I. Baida, A. Belkhir, D. Van Labeke, O. Lamrous "Subwavelength metallic coaxial waveguides in the optical range: Role of the plasmonic modes," Phys. Rev. B **74,** 205419 (2006).
34. E. D. Palik "Handbook of Optical Constants of Solids," New York: Academic, 1985.
35. K. J. Webb and J. Li "Analysis of transmission through small apertures in conducting films," Phys. Rev. B **73,** 033401 (2006).
36. S. I. Bozhevolnyi, J. Erland, K. Leosson, P. M. W. Skovgaard, and J. M. Hvam "Channel Plasmon-Polariton Guiding by Subwavelength Metal Grooves," Phys. Rev. Lett. **95**, 046802 (2005).
37. S. I. Bozhevolnyi, V. S. Volkov, E. Devaux, J.-Y. Laluet, and T. W. Ebbesen "Channel plasmon subwavelength waveguide components including interferometers and ring resonators," Nature **440**, 508 (2006)
38. S. I. Bozhevolnyi, "Effective-index modeling of channel plasmon polaritons," Opt. Express **14,** 9467 (2006).
39. J. D. Jackson, *Classical Electrodynamics*, Third Ed., sec. 8.6, (John Wiley & Sons, New York, 1998).

1. Introduction

Nanoscale apertures in a metal show astonishing optical properties leading to enhanced and selective light transmission [1, 2], and light confinement [3, 4]. Several structures are considered. Efficient light transmission through a single subwavelength aperture in a metallic film can be achieved by optical tunneling through the fundamental guided mode in the hole. The key role

#78453 - $15.00 USD Received 22 December 2006; revised 2 February 2007; accepted 6 February 2007

of the aperture geometry on the light transmission process has been demonstrated experimentally [5, 6, 7] and theoretically [8, 9, 10, 11]. The design of such subwavelength metal apertures is still a major challenge for the conception of optimal probes for scanning near-field optical microscopy [12]. Indeed light confinement in tiny apertures has allowed an impressive enhancement of single-molecule analysis by fluorescence detection in subwavelength holes [3, 13].

Enhanced light transmission is also achieved through metallic films with arrays of subwavelength holes [1]. In this last case, the optical tunneling through the holes is boosted by the excitation of surface plasmon polaritons (SPP) on the flat metallic surfaces [14, 15]. However, the dispersion properties of surface waves are also strongly dependent on the hole geometry [16, 17]. The role of the shape and size of each aperture on the transmission resonance has been evidenced experimentally by several groups [18, 19, 20, 21]. Another very recent example of the crucial role of the aperture geometry on the optical properties of such structures is the enhancement of the nonlinear optical response of metallic films with hole arrays [22]. This properties are attributed to slow modes due the cut-off behaviour in each hole. In hole arrays, apertures act as uncoupled metallic waveguides due to the opacity of noble metals in the visible and infrared wavelength range if the metal thickness is greater than the penetration depth of the electromagnetic field (about 25 nm). Consequently, the optical modes of the holes can be studied independently in a each aperture.

In previous theoretical studies of light transmission through single holes or through hole arrays in metallic films, several approaches have been used to modelize the electromagnetic field in the apertures. The simpler model makes use of perfect metallic walls [9, 23, 14], which can be modified with an effective hole radius [24]. Alternatively, time consuming numerical methods allow accurate calculations of optical modes and light transmission (Fourier decomposition [15, 20, 25], FDTD [26], or finite elements [27]). Optical modes in cylindrical holes can be calculated by well-known waveguide theory [28, 29, 30], whereas approximation methods have been proposed recently for rectangular [31] and circular [32] metallic waveguides. Numerical methods allow to study other hole geometries [33]. However, these approaches do not allow to clearly distinguish the respective role of the hole shape, hole size, and metal permittivity. Here, we develop analytical formulae for the effective index of the fundamental optical guided mode in rectangular nanoscale holes. It provides simple physical interpretations of the influence of the shape and size of the holes, and the role of the finite permitivitty of the metal. The penetration depth of the electromagnetic field in the metallic walls and the role of coupled surface plasmon polaritons are emphasized.

In this article, we focus on the fundamental modes of 1D and 2D subwavelength metallic waveguides. We develop explicit analytical expressions for the 1D and 2D effective indices, in excellent agreement with numerical computations on broad size and wavelength ranges. In the first part, we study the fundamental TM mode of 1D planar metallic waveguides. This mode is composed of two coupled surface plasmon polaritons. We show that this coupling is driven by the metal skin depth and the waveguide width, leading to a wavelength independent effective index in the near- and mid-infrared wavelength. These results have important consequences in nanoscale hole waveguides. In the second part, we focus on 2D subwavelength rectangular metallic waveguides. We provide simple analytical equations for the effective index of the fundamental TE mode. Our model takes into account losses, and is in very good agreement with 2D finite element calculations. The role of coupled surface plasmon polaritons and metal skin depth on the effective index is analyzed. We propose very simple expressions for the effective index n and the cut-off wavelength λ_c of the fundamental guided mode. Taking into account the finite permittivity of the metal induces a red-shift of the cut-off wavelength of the fundamental guided mode of rectangular waveguides. The nanoscopic origin of this phenomenon is described. Universal curves of the effective index and the cut-off frequency of any rectangular

#78453 - $15.00 USD Received 22 December 2006; revised 2 February 2007; accepted 6 February 2007

metallic waveguide are presented. These results provide a straightforward analysis of the optical properties of nanoscale apertures, and a tool for the design of efficient metallic structures for extreme light confinement.

2. Coupled surface plasmon polaritons 1D metallic waveguides

We first study a one dimensional metallic waveguide. A dielectric slab of permittivity ε_d and width w is surrounded by two semi-infinite metallic regions of permittivity ε_m (see Fig. 1(a)). In the following, the subscripts d and m denote the dielectric and metallic regions, respectively. κ is the wavenumber of the fundamental guided mode, and $k_0 = 2\pi/\lambda$ is the free space wavenumber.

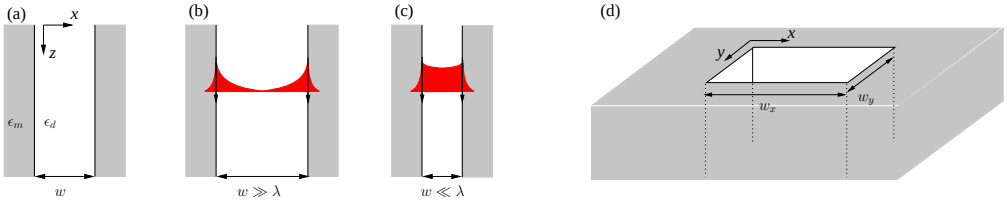

Fig. 1. Schematic of 1D planar metallic waveguide (a) and 2D rectangular metallic waveguide (d). The fundamental TM mode of planar 1D waveguides is composed of two surface plasmons waves (red). They are weakly coupled in wide waveguides ($w \gg \lambda$, (b)) and strongly coupled in narrow waveguides ($w \ll \lambda$, (c))

In case of perfect metallic walls, the fundamental waveguide mode is a TEM mode whose axial wavenumber is $\kappa = \sqrt{\varepsilon_d} k_0$. κ is independent of the waveguide width w, and there is no cut-off frequency. In case of non-perfect metal, the exact 1D mode equation for even TM modes in the waveguide is given by:

$$\frac{k_{xd}}{\varepsilon_d}\left[\frac{1-e^{ik_{xd}w}}{1+e^{ik_{xd}w}}\right] + \frac{k_{xm}}{\varepsilon_m} = 0 \tag{1}$$

where $k_{xd} = \sqrt{\varepsilon_d k_0^2 - \kappa^2}$ and $k_{xm} = \sqrt{\varepsilon_m k_0^2 - \kappa^2}$.

In the limit of wide waveguides ($w \gg \lambda$), an approximate solution is obtained for the fundamental TM_0 mode. When $|\Im(k_{xd}w)| \gg 1$, Eq. (1) is reduced to $\frac{k_{xd}}{\varepsilon_d} + \frac{k_{xm}}{\varepsilon_m} = 0$, which is the exact relation dispersion of surface plasmon polaritons (SPP) on a single semi-infinite dielectric/metal interface. The effective index of this mode is $n_{eff} = \frac{\kappa}{k_0} = \frac{1}{\sqrt{\frac{1}{\varepsilon_d}+\frac{1}{\varepsilon_m}}}$. The fundamental TM mode is composed of two uncoupled surface plasmon polaritons propagating along both dielectric/metal interfaces (see fig. 1(b)).

For very narrow (sub-wavelength) waveguides, the coupling between both SPP can not be neglected anymore. When $|k_{xd}w| \ll 1$, $\frac{1-e^{ik_{xd}w}}{1+e^{ik_{xd}w}} \sim -ik_{xd}w/2$ and Eq. (1) becomes

$$\frac{k_{xm}}{\varepsilon_m} = \frac{k_{xd}}{\varepsilon_d}\left(\frac{ik_{xd}w}{2}\right). \tag{2}$$

With $k_{xd}^2 - k_{xm}^2 = (\varepsilon_d - \varepsilon_m)k_0^2$ we can deduce the mode equation as a function of k_{xd}:

$$k_{xd}^2\left[1 + k_{xd}^2\left(\frac{\varepsilon_m}{\varepsilon_d}\right)^2\frac{w^2}{4}\right] = (\varepsilon_d - \varepsilon_m)k_0^2 \tag{3}$$

#78453 - $15.00 USD Received 22 December 2006; revised 2 February 2007; accepted 6 February 2007

and we obtain a simple, analytical expression for the effective index of the fundamental TM_0 mode (coupled SPP approximation):

$$n_{1D} = \frac{\kappa}{k_0} = \sqrt{\varepsilon_d}\left(1 + \frac{\lambda}{\pi w\sqrt{-\varepsilon_m}}\sqrt{1+\frac{\varepsilon_d}{-\varepsilon_m}}\right)^{1/2} \tag{4}$$

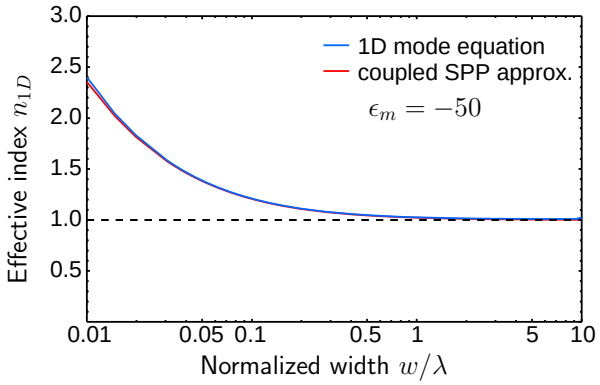

Fig. 2. Effective index of the fundamental TM mode of a planar metallic waveguide ($\varepsilon_d = 1$) as a function of the width w for $\varepsilon_m = -50$.

The expression $\frac{\lambda}{\pi w\sqrt{-\varepsilon_m}}\sqrt{1+\frac{\varepsilon_d}{-\varepsilon_m}}$ in Eq. (4) is a correction term due to the coupling of surface plasmon polaritons. Fig. 2 shows the comparison of the calculation of n_{1D} with Eq. (4) and with the exact mode equation (1) for $\varepsilon_m = -50$. The effective index is plotted as a function of the normalized width w/λ. Importantly, for very narrow waveguides ($w < 0.1\lambda$) the increasing coupling between both surface plasmon polaritons induces a strong increase of the effective index. For greater values of w/λ, the results are always close to the perfect metal solution ($n_{1D} \sim \sqrt{\varepsilon_d}$). Hence, no deviation occurs between the approximated and the exact solutions for large waveguides, even if the approximation was supposed to be most valid for very narrow waveguides. As a result, a very good agreement is achieved on a broad size range (three orders of magnitude).

Equation (4) can be simplified in two ways. First, the term $\sqrt{1+\frac{\varepsilon_d}{-\varepsilon_m}}$ can be omitted as soon as $|\varepsilon_m| \gg \varepsilon_d$. Second, using a Drude model for the metal permittivity allows to write a very compact expression for n_{1D}:

$$n_w = \sqrt{\varepsilon_d\left(1+\frac{2\delta_c}{w}\right)} \tag{5}$$

where $\delta_c = \frac{c}{\omega_p}$ is a good approximation for the metal skin depth within the Drude model $\varepsilon_m = 1 - \frac{\omega_p^2}{\omega^2 + i\omega\gamma}$ where $\omega = k_0 c$ is the frequency. Precisely, Eq. (5) is valid when $\gamma \ll \omega \ll \omega_p$. For high conductivity metals (Ag, Au, Al), this corresponds to the near- and mid-infrared (NIR-MIR) range. In the following we use $\omega_p = 1.2\times10^{16}$ s^{-1} and $\gamma = 1.2\times10^{14}$ s^{-1} as a good approximation for the permittivity of gold [34] (the dielectric region is air, $\varepsilon_d = 1$). We obtain $\delta_c \sim 25$ nm. The difference between the skin depth and δ_c is less than 14% in the 0.5 μm to 20 μm wavelength range, as illustrated on fig. 3.

The comparison of expressions (4) and (5) with exact mode calculation and with single SPP approximation is given on fig. 4 for both real and imaginary parts of the effective index n_{1D}. The waveguide width is $w = 100$ nm. A very good agreement between the 1D mode equation (1)

#78453 - $15.00 USD Received 22 December 2006; revised 2 February 2007; accepted 6 February 2007

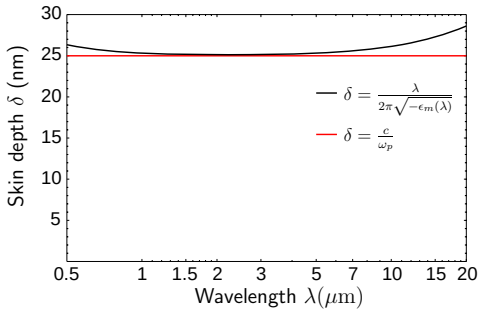

Fig. 3. Skin depth of the metal $\delta = \lambda/(2\pi\sqrt{-\varepsilon_m(\lambda)})$ (dark) as a function of the wavelength. The skin depth is nearly constant and equal to $\delta = c/\omega_p$ (red) between 0.5 and 20 μm.

and the coupled SPP approximation (Eq. (4)) is obtained for wavelengths greater than 1 μm, for both the real and imaginary parts of the effective index. In this example, the condition $|k_{xd}w| \ll 1$ is no more fullfilled below 1 μm. As a result, a slight discrepancy is found between the 1D mode equation and the coupled SPP approximation. On fig. 4, the effective index of the planar metallic waveguide is also compared to the effective index of a single SPP, and to the constant effective index n_w given by Eq. (5).

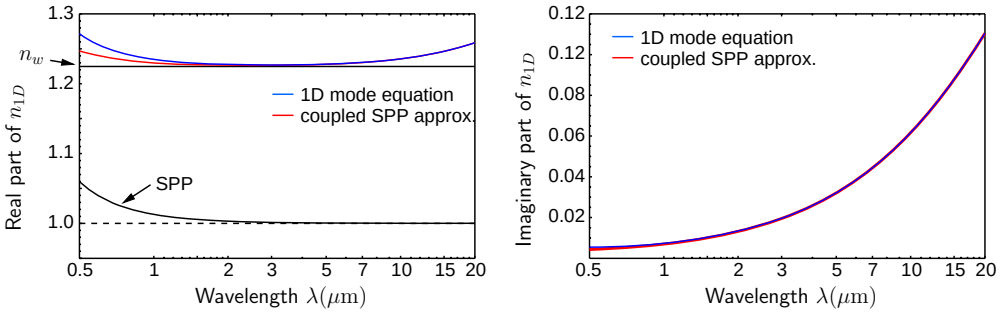

Fig. 4. Real (left) and imaginary (right) parts of the effective index of the fundamental TM mode of a planar metallic waveguide as a function of the wavelength λ. Dark solid line: effective index of a single metal/dielectric surface plasmon polariton. The metal permittivity is given by a Drude model: $\varepsilon_m = 1 - \frac{\omega_p^2}{\omega^2 + i\omega\gamma}$, $\omega_p = 1.2 \times 10^{16}\mathrm{s}^{-1}$, $\gamma = 1.2 \times 10^{14}\mathrm{s}^{-1}$. The waveguide width is $w = 100$ nm.

Let us emphasize the main properties of the effective index n_{1D}. The real part of n_{1D} is much greater than the effective index of a single SPP, due to the strong coupling between both SPP. The coupling mechanism between both SPP can be expressed by the ratio between the metal skin depth and the waveguide width δ/w. As a result, the constant metal skin depth induces a constant effective index n_w given by Eq. (5). It provides an accurate evaluation of the real part of n_{1D} in the $1-10$ μm wavelength range (see fig. 4).

Equation (5) gives a very simple relation for the increase of the effective index when decreasing the distance between metal walls. This phenomenon induces a gradient of the effective index in V-shaped metal grooves, and allows light to be confined at the bottom of the groove. This light confinement mechanism has led to the achievement of channel plasmon-polariton waveguides made of subwavelength metal grooves [36, 37, 38].

#78453 - $15.00 USD Received 22 December 2006; revised 2 February 2007; accepted 6 February 2007

3. 2D rectangular metallic waveguides

We now consider a 2D rectangular metallic waveguide (fig. 1(d)) with $w_x > w_y$ and $\lambda \gg w_x, w_y$: the NIR-MIR wavelength range is above the cut-off wavelength. We focus our study on the TE $_{10}$ mode. This mode has the smallest attenuation along the waveguide, and it has been shown that it should play a predominent role in the enhanced transmission through subwavelength holes in a metallic film [14]. Recently, Gordon et al. have shown that for good metals this 2D problem can be approximated by two 1D problems, leading to accurate evaluation of the cut-off wavelength of rectangular metallic waveguides [31]. In the following, we use a similar approach to provide analytical formulae for the effective index of waveguide modes. Both 1D problems are described by mode equations of 1D metallic waveguides, which are simplified by first order approximations. We emphasize that absorption losses in metal are included in the model. It can be noted that an alternative approach based on perturbation of boundary conditions and Green's theorem was described by Jackson [39]. However, we found that our model provides slightly different and more accurate results. Moreover, simple equations allow us to discuss the role of coupled surface plasmon polaritons, and of metal skin depth.

3.1. Analytical expression of TE$_{10}$ *modes*

In case of perfect metal, the wavenumber of the TE $_{10}$ mode is $\kappa_0 = \sqrt{\varepsilon_d k_0^2 - \frac{\pi^2}{w_x^2}}$, and this mode can be decomposed by two plane waves whose wavevectors are in the (x,z) plane. In case of good (but non perfect) metal, the TE $_{10}$ mode can be decomposed by two pairs of coupled surface plasmons propagating in (x,z) planes at $y = 0$ and $y = w_y$ [31]. Hence, its axial wavenumber κ can be calculated by the equation of the symmetric transverse electric TE $_1$ mode of a planar metallic waveguide, replacing the dielectric permittivity ε_d by an effective permittivity $\varepsilon'_d = n_{1D}^2$ where n_{1D} is the effective index of coupled SPP, given by Eq. (4). The TE $_1$ mode equation can be written:

$$\tan(k_{xd} w_x/2) = i\frac{k_{xm}}{k_{xd}} \tag{6}$$

Using a first order approximation of the tan function at $k_{xd} = \frac{\pi}{w_x}$, and using $k_{xd}^2 - k_{xm}^2 = (\varepsilon'_d - \varepsilon_m)k_0^2$, we find that the effective index of the 2D TE $_{10}$ mode can be written:

$$n_{2D} = \frac{\kappa}{k_0} = \sqrt{\varepsilon'_d - \left(\frac{\lambda}{2w'_x}\right)^2} \tag{7}$$

where the effective width w'_x is given by:

$$w'_x = w_x \left(1 + \frac{\lambda}{\pi w_x \sqrt{(\varepsilon'_d - \varepsilon_m) + \left(\frac{\lambda}{2w_x}\right)^2}}\right) \tag{8}$$

The analytical formulae (Eq. (7) and (8)) obtained for the effective index of the TE $_{10}$ of 2D rectangular waveguide modes are compared to finite element calculations made with a commercial software [27] on fig. 5. The results are also compared to the perfect metal solution. The role of the exact metal permittivity is clearly shown. A perfect agreement between our analytical formulae and finite element calculations shows the accuracy of our approximations. We point out that the influence of the metal permittivity can not be taken into account by simply introducing an effective width [24]. The coupling of surface plasmon polaritons plays a key role. Both effective dielectric permittivity ε'_d and effective width w'_x are necessary to achieve a quantitative agreement with finite element calculations.

#78453 - $15.00 USD Received 22 December 2006; revised 2 February 2007; accepted 6 February 2007

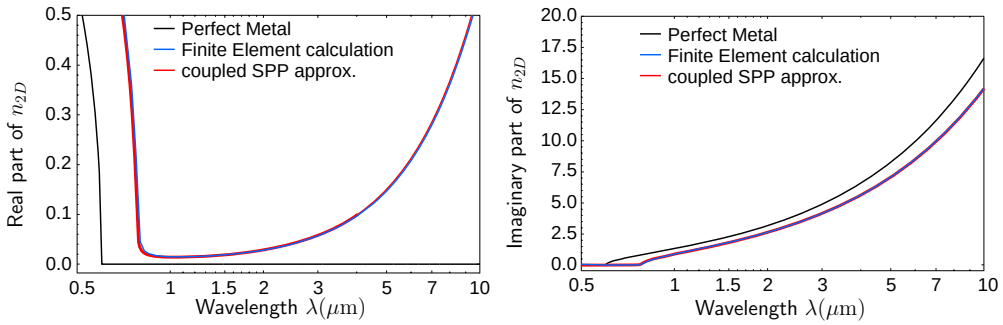

Fig. 5. Real (left) and imaginary (right) parts of the effective index of the fundamental TE_{10} mode of a rectangular metallic waveguide as a function of the wavelength λ. The widths of the waveguide is $w_x = 300$ nm and $w_y = 200$ nm. The results of the perfect metal (dark), finite element calculation (blue) and coupled SPP approximation (Eq. (7) and (8)) (red) are compared.

3.2. *Role of the metal skin depth*

Since we study subwavelength waveguides ($w_x < \lambda$) and $\varepsilon_d' \ll |\varepsilon_m|$, it can be shown easily that the effective width w_x' can be approximated by:

$$w_x' = w_x + 2\delta \tag{9}$$

where δ is the metal skin depth defined previously. We have calculated the imaginary part of n_{2D} with Eq. (7) and (9). Once again, the results are in quantitative agreement with finite element calculations (the results are not shown on fig. 5 since both curves are superimposed).

In the following, we neglect the imaginary part of the metal permittivity. Hence, the role of the metal on the effective index can be taken into account only by its constant skin depth in the NIR-MIR frequency range, leading to a very simple expression for the effective index n_{2D} of the TE_{10} mode :

$$n_{2D} = \sqrt{\varepsilon_d \left(1 + \frac{2\delta}{w_y}\right) - \left(\frac{\lambda}{2(w_x + 2\delta)}\right)^2} \tag{10}$$

Equation (10) provides a very simple interpretation of the effect of the metal skin depth on the fundamental guided mode TE_{10}. Importantly, the penetration depth of the electromagnetic field in the metal δ does not play the same role on the different metallic walls of the waveguide. On the *x*-direction, we have shown that an effective width can be defined, simply increasing the waveguide width w_x by 2δ. On the *y*-direction, the effect of the finite permittivity of the metal is due to coupled surface plasmon polaritons, and is only sensitive for widths not greater than a few δ.

3.3. *Red-shift of the cut-off wavelength due to the finite permittivity of the metal*

From Eq. (10) we deduce the expression of the cut-off wavelength λ_c of rectangular waveguides as a function of the widths w_x and w_y and of the skin depth δ :

$$\lambda_c = 2(w_x + 2\delta)\sqrt{\varepsilon_d \left(1 + \frac{2\delta}{w_y}\right)} \tag{11}$$

Equation (11) gives a straightforward interpretation of the red shift of the cut-off wavelength due to the finite permittivity of the metal. This effect may be responsible for the red shift of

#78453 - $15.00 USD Received 22 December 2006; revised 2 February 2007; accepted 6 February 2007

the transmission peak observed through single apertures in metal [7, 9, 10, 11, 31]. In each metallic walls, the increase of the penetration of the electromagnetic field increases the cut-off wavelength. However, the importance of this effect is not the same on each direction, as stated before for the effective index.

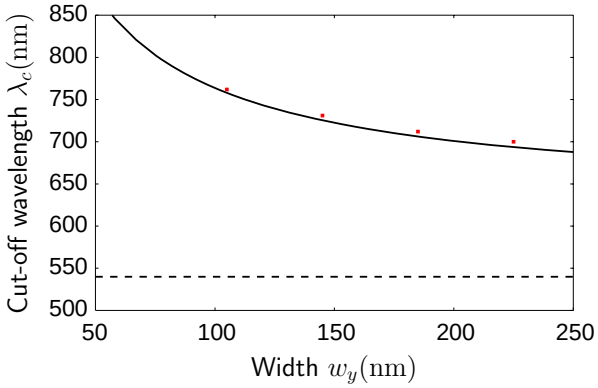

Fig. 6. Cut-off wavelength of the fundamental guided mode TE_{10} as a function of w_y, for a silver rectangular waveguide with $w_x = 270$ nm. The approximated model from Eq. (11) (solid curve) is compared to reference [31] (red points), and to the perfect metal case (horizontal dashed line).

This red-shift is illustrated on fig. 6. The cut-off wavelength λ_c is plotted as a function of w_y for a silver rectangular waveguide with $w_x = 270$ nm. The results are in very good agreement with reference [31] (red points). They show the influence of coupled surface plasmon polaritons for small w_y. In this example $\delta = 23$ nm. The cut-off wavelength of perfect metal waveguides would be constant and equal to 540 nm (dashed line).

3.4. *Universal curves for the effective index*

Normalizing dimensions and wavelengths to the metal skin depth δ in Eq. (10) allows to plot universal curves for the effective index of the fundamental guided mode TE_{10}. The results are valid for any rectangular metallic waveguide (for most noble metals in the NIR-MIR frequency range $\delta \simeq 25$ nm). This is illustrated on fig. 7 for three different wavelengths.

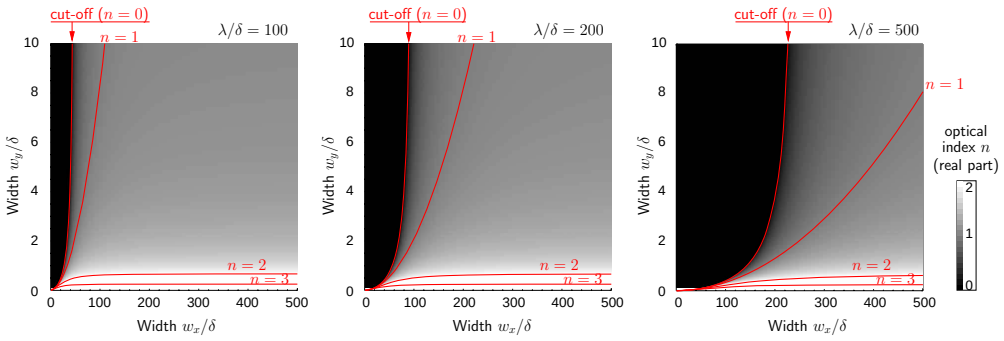

Fig. 7. Universal curves for the real part of the effective index of the fundamental guided mode TE_{10} for three different wavelengths (λ/δ = 100, 200 and 500). Dimensions of the rectangular waveguide (w_x,w_y) are normalized to the metal skin depth δ.

#78453 - $15.00 USD Received 22 December 2006; revised 2 February 2007; accepted 6 February 2007

On fig. 7, we clearly distinguish three different propagating conditions. In the dark region there is no propagating modes. From Eq. (10), we also note that in this case, for $\lambda \ll w_x$, the attenuation length along the propagation direction z becomes independent of the wavelength and equal to: $\Lambda = (w_x + 2\delta)/\pi$. This property is particularly important for the design of 'zero-mode' metallic waveguides for single-molecule fluorescence analysis in tiny volumes [13, 3].

The grey region corresponds to classical waveguiding conditions with effective indices close to 1. The white region corresponds to very small values of w_y, and clearly shows the increase of the effective index due to the coupling between surface plasmon polaritons. As demonstrated previously (see Eq. 10), this effect is only sensitive when w_y is of the same order than δ.

3.5. Universal curves for the cut-off wavelength

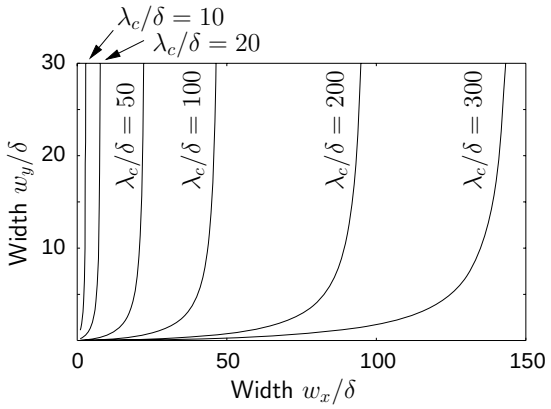

Fig. 8. Universal curves for the cut-off wavelength of the fundamental guided mode TE_{10} of rectangular metallic waveguides. Dimensions and wavelengths are normalized to the metal skin depth δ.

Using the same normalization procedure in Eq. (11), we have also plotted universal curves for the cut-off wavelength of the fundamental guided mode TE_{10} for any rectangular metallic waveguide (see fig. 8). These curves give the waveguide geometries (w_x, w_y) which provide a given cut-off wavelength λ_c. They show that the effect of coupled surface plasmon polaritons on the cut-off wavelength is sensitive up to about $w_y/\delta = 10$. For large values of w_y, the cut-off wavelength limit is equal to $2(w_x + 2\delta)$.

4. Conclusion

In this paper, we have studied the fundamental optical modes of 1D and 2D subwavelength metallic waveguides. We have proposed a simple model based on coupled surface plasmon polaritons and first-order approximations. Analytical expressions have been developped, and are in very good agreement with numerical calculations. This approach reveals the role of non-perfect metallic walls on optical modes. These effects can be taken into account by introducing the metal skin depth, leading to very simple expressions for the effective index n and the cut-off wavelength λ_c of the fundamental guided mode. Universal curves of n and λ_c for any rectangular metallic waveguide have been presented. They provide a simple way to evaluate the role of the metal and of the geometry of nanoscale apertures on their optical properties. This model should be an efficient tool to design new metallic structures for the enhancement of single-molecule analysis in subwavelength apertures [13, 3], and nonlinear optical effects in metallic films [22].

#78453 - $15.00 USD Received 22 December 2006; revised 2 February 2007; accepted 6 February 2007

Acknowledgements

The authors are grateful towards Philippe Lalanne for stimulating discussions, and Lorenzo Bernardi for assistance in simulation tools.

#78453 - $15.00 USD Received 22 December 2006; revised 2 February 2007; accepted 6 February 2007